Symmetrical Bioinspired UWB Camellia Flower-Shaped Monopole Antenna

Rodrigo César Fonseca da Silva, Elder Eldervitch Carneiro de Oliveira, Pedro Carlos de Assis Júnior, Glauco Fontgalland and Tales Augusto Carvalho de Barros

***Abstract* — A new planar multilateral bioinspired monopole antenna for Ultra-Wideband (UWB) application is proposed. Experimentally confirmed, the proposed antenna has wide impedance bandwidth, covering from 2.56 GHz to more than 11 GHz. Although the proposed antenna has a complex structure, it is easy to design and fabricate. The mathematical process, Gielis transformation, used to elaborate the symmetry is described and the design is demonstrated assuming FR4 substrate with a relative dielectric constant of 4.4 and thickness of 1.6 mm. The main electromagnetic parameters of the antenna are simulated for the UWB operation and compared with the experimental results obtained from the built prototype. Details of the results of the proposed antenna are presented and discussed.**

Keywords — ***Bioinspired monopole antenna, coordinate transformation, Gielis formula, planar antenna, ultra-wideband.***

I. INTRODUCTION

The antenna is the fundamental element for the radio communication entity by means of radio frequency and microwave. Currently, there is a demand in the search for greater bandwidth, multiband, and low profile antennas for both commercial and military purposes. In the last decades, with the increasing expansion and modernization of the wireless communication systems, the antennas have been highlighted as a crucial component in this scenario of development. Modern telecommunication systems increasingly require the miniaturization of devices, which must operate in multiband, present low cost, and easy to manufacture [1], [2].

In this context, microstrip patch antennas are an excellent option due to their advantages. They have many attractive features such as low profile, lightweight, ease of fabrication, and allowing both linear and circular polarization [1] – [3]. However, an antenna with a patch element with canonical form has a low directivity value and generally exhibits a broad radiation pattern, which constraints its use in systems requiring long distance communication. The solution to this type of problem is to find new antenna's design providing radiation concentration in a specific region in the space, i.e., increase the antenna's directivity, which can be obtained by modifying its geometric dimensions [3].

Rodrigo C. F. da Silva, Elder E. C. de Oliveira and Pedro C. A. Júnior, State University of Paraíba, Rua Alfredo Lustosa Cabral, S/N, CEP: 58706-560, Patos – PB, Brazil. Glauco Fontgalland, Federal University of Campina Grande, Rua Aprígio Veloso, 882 – Bairro Universitário, Campina Grande - PB, CEP: 58429-900. Tales Augusto Carvalho de Barros, Federal Institute of Paraíba Av. João da Mata, 256 - Jaguaribe, João Pessoa - PB, CEP: 58015-020. E-mails: r.c.fonseca@uepb.edu.br, elder2@ymail.com, pedro_fisica2005@yahoo.com.br, fontgalland@dee.ufcg.edu.br, talesuepbfisica@gmail.com.

The electrical properties of the printed monopole antennas (PMA) depend on the geometry of both the monopole element, the substrate, and the ground plane. A monopole element may be electrically short (length << ¼ λ) or quasi-resonant (length ~ ¼ λ), and may be thin (length-to-radius ratio > 10^4) or relatively thick (length-to-radius ratio between 10 and 10^4) [4]. The substrate is function of the permittivity and permeability, which can be homogeneous or inhomogeneous, isotropic or anisotropic, linear or nonlinear, single layer or multilayers filling completely or partially the volume around the antenna and/or ground plane. The ground plane, in its turn, can completely or partially be filled and present a variety of designs, such as DGP (defect ground plane), PBG (photonic band gap), fractals, metasurface, etc. Keeping in mind the needs for a lightweight, easy to fabricate, environmentally friend, high directive, low profile, and low cost antenna, this article presents a PMA with a bioinspired innovate geometry similar to the flower of the Camellia operating in the Ultra-Wideband (UWB, 3.1-10.6 GHz) and Wireless Local Area Network (WLAN, 5-6 GHz) [5], [6].

This paper is divided into three sections besides the introduction. In Section 2, the used methodology, materials, and methods to design a geometrically bioinspired antenna are presented. In the Section 3, the simulated and measured antennas are presented and the conclusions are given in Section 4.

II. METHODOLOGY: MATERIALS AND METHODS

Nowadays, several technologies stand out in obtaining geometric representation of the forms found in nature. We can cite fractal geometry, the Fibonacci series, the golden ratio, the Gielis formula, and plant-based design for antennas [7], [8]. The description of the properties of complex energy conversion processes in plant-shaped devices, as well as their similarity to parabolic reflector structures when absorbing electromagnetic waves can be found in refs. [9], [10].

The bioinspired geometric design used in this work was developed from a coordinate transformation of the cartesian axis, which can be seen in Fig. 1 and Fig. 2. With this procedure, one can obtain a symmetrical flower shape, similar to a camellia flower, whose structure will be used in the modeling of the proposed microstrip antenna. Several operating parameters of an antenna, such as resonance frequency, bandwidth, gain, and radiation pattern, are directly affected by its geometry and the materials used in its construction. Consider Ox and Oy, the primitive axes of the cartesian axis system coordinates with origin O(0,0). Now, let Ox_1 and Oy_1 be the new coordinate axis after the primitive system has been rotated from an angle θ around the origin. Let P(x,y) be any point in the primitive system. Therefore, the same point P will have coordinates P(x_1,y_1), relative to the new system, satisfying the transformation in the rotational equations, in $\mathbf{R}^2$.

$$\begin{pmatrix} x \\ y \end{pmatrix} = [M]_\theta \begin{pmatrix} x_1 \\ y_1 \end{pmatrix} \qquad [M]_\theta = \begin{pmatrix} \cos\theta & -\sin\theta \\ \sin\theta & \cos\theta \end{pmatrix} \tag{1}$$

The Eq. (2) is known in the literature as a rotation matrix by an angle θ [11]. Fig.1 shows the result of the application of 7 successive rotations of an ellipse, of $\theta = \pi/4$. Around the origin of the Cartesian axis. For the dielectric substrate, the material chosen was the FR4 (glass fiber), combined with thickness of the dielectric, h = 1.5 mm, loss tangent of ($tan\delta$) 0.02, and electrical permittivity, ε_r = 4.4.

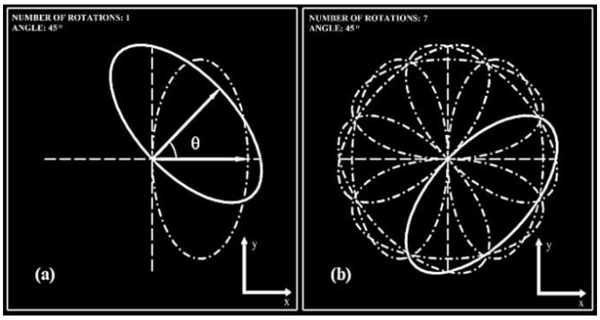

Fig. 1. Bioinspired symmetry, from the translation of an ellipse around the origin: (a) Determination of the axis of rotation with $\theta = \pi/4$ developed with a MAPLE® routine. (b) Structure obtained after 7 successive rotations.

The Fig.2 illustrates the structure of the proposed antenna. The antenna was produced by filling the total area obtained by the mathematical process in Fig.1a. A partial ground plane with a rectangular slot on the top side was used to control the impedance matching [12] – [14]. This slot plays an important role in obtaining UWB behavior.

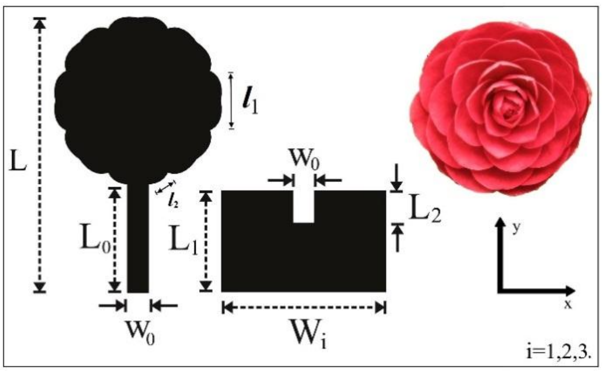

Fig. 2. Elliptical Camellia shape, characterized by the union of the areas of the 7 ellipses. Parameters: L=36.70 mm, L_0=14.50 mm, L_1=13.50 mm, L_2=4,33 mm, l_1=10.08 mm, l_2=3.179 mm,W_0= 2.83 mm, W_1=22.00 mm, W_2=30.00 mm, W_3=35.00 mm and perimeter P=70.056 mm.

In [13] it's indicated that the lowest frequency in the impedance bandwidth of the antenna is directly influenced by the perimeter p and by effective permittivity of the dielectric ε_{eff} according to equations

$$f_L(GH_Z) = 300/\left(p\sqrt{\varepsilon_{eff}}\right) \tag{2}$$

$$\varepsilon_{eff} \approx (\varepsilon_r + 1)/2 \tag{3}$$

III. EXPERIMENTAL AND SIMULATED RESULTS

The numerical simulations were conducted on the crescent-width ground plane using the commercial software Ansoft Designer™. The measurements of the prototypes were performed in the Antenna Laboratory of the Federal Institute of Paraiba with a vector network analyzer model R&S ZVB14. The parametric studies of the effect of the ground plane base width on reflection coefficient are shown in Fig. 3.

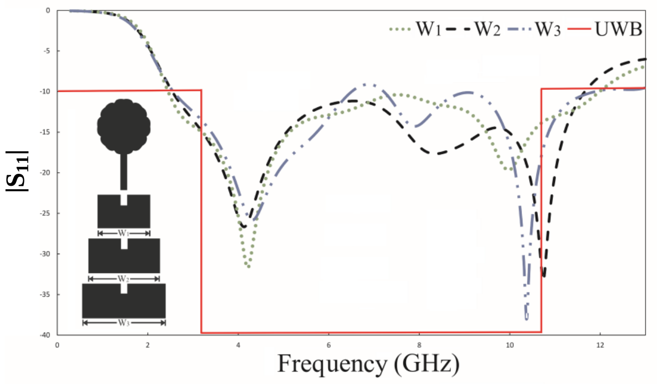

Fig. 3. Simulated reflection coefficient parameter for the proposed antenna with various lengths of the ground plane.

The simulated W_1 and W_2 antennas presented the UWB behavior, with bandwidths BW_1 = 9.32 GHz and BW_2 = 9.29 GHz, respectively. In addition, the W_3 antenna presents a good result for simulated reflection coefficient from 2.57 GHz – 6.52 GHz, approximately, with possible application in range WLAN and 7.21 GHz - 11.91 GHz, with possible applications in IEEE X-BAND. However, this parametric study proves that changes in the width of the ground plane base can compromise the UWB behavior of the PMA (Elliptical Camellia monopole antenna). To validate this study, we constructed a prototype with the dimensions of W_2, which presented the best performance in the simulations and the UWB band became more evident, see Fig.3.

TABLE I: SIMULATED RESULTS FOR THE PMA BANDWIDTH ($|S_{11}| \leq$ -10 dB)

Simulated Antennas	Frequencies (GHz)		
	f_L	f_h	UWB
W_1	2.4611	11.7795	9.3184
W_2	2.4738	11.7668	9.2930
Simulated Antenna	Bandwidth: $f_h - f_L$ (GHz)		
W_3	2.5755 – 6.5165	7.2157 – 11.9067	

Fig. 4 shows the comparison between the measured and simulated values for the antenna W_2. Using Eq. (1), we found f_L~ 2.5 GHz, which agrees with the simulated value. It is possible to notice a good agreement between theoretical and experimental data.

TABLE II: SIMULATED AND MEASURED FOR THE PMA BANDWIDTH ($|S_{11}| \leq$ -10 dB)

Antenna	Frequencies (GHz)		
	f_L	f_h	UWB
Simulated W_2	2.4738	11.7668	9.2930
Measured W_2	3.1700	13.5000	10.330

The discrepancy in the low frequencies, which can be viewed in the Table II, is mostly due to the small ground plan, substrate, and difficulties in obtaining the millimeter details of the PMA structure through the chemical process of corrosion of the FR4 substrate.

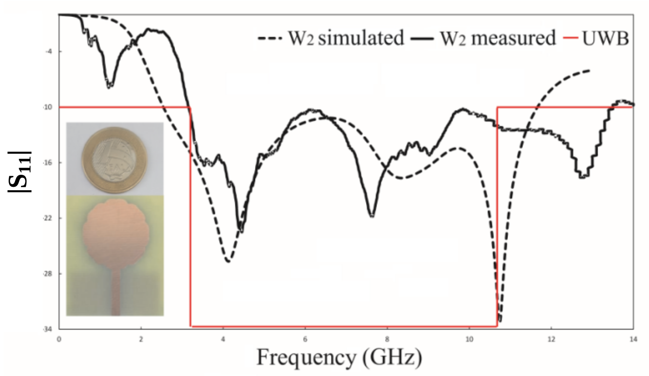

Fig. 4. Simulated and measured reflection coefficient parameter of the PMA "*Elliptical Camellia*" for W_2.

Fig. 5 to 7 show, respectively, the 2-D and 3-D simulated radiation patterns at three peaks of ressonances of the PMA: f_1 = 4.1392 GHz, f_2 = 8.3980 GHz and f_3 = 10.7371 GHz, of the geometrically bioinspired PMA antenna, where the index (1,2,3) represents each resonance frequency.

In Fig. 5, it can be observed that the directive gain is stable from θ_1 = -148.00º to θ_1 = 150.00º, where the maximum gain of 1.98 dBi occurs in the broadside direction, backward radiation is bellow of -10 dB, *E*-plane front-to-back ratio is *F/B*= 0.7478 and half power bandwidth (HPBW) = 298.00º.

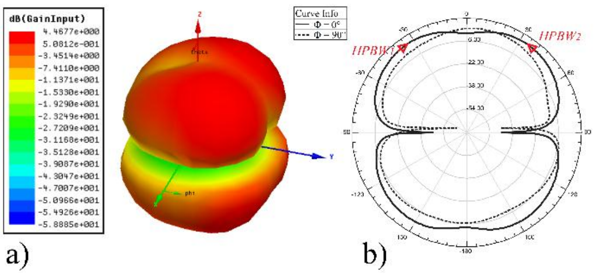

Fig. 5. Simulated radiation pattern for f_1 = 4.1392 GHz: Field 3-D with gain in dBi. b) Field 2-D with gain in dBi.

The Fig. 6 shows that the gain is also stable from θ_2 = -129.00º to θ_2 = 127.00º, where the maximum gain of -0.69 dBi, backward radiation of -7.2873 dB, *F/B*= 0.4492 and (HPBW) = 256.00º.

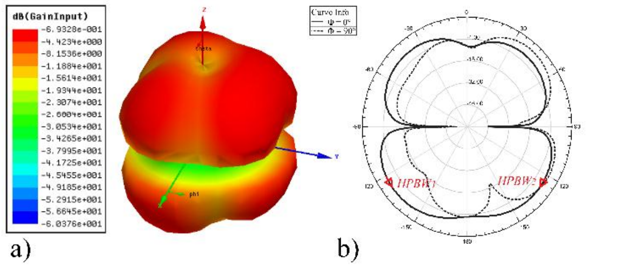

Fig. 6. Simulated radiation pattern f_2 = 8.3980 GHz: a) Field 3-D with gain in dBi. b) Field 2-D with gain in dBi.

In the Fig. 7, the gain is stable from θ_3 = -33.00º to θ_3 = 34.00º, where the maximum gain of 7.10 dBi, backward radiation of -3.5670 dB, *F/B*= 11.3075 and (HPBW) = 67º.

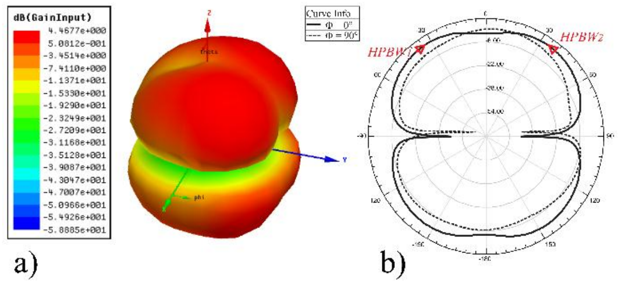

Fig. 7. Simulated radiation pattern f_3 = 10.7371 GHz: Field 3-D with gain in dBi. b) Field 2-D with gain in dBi.

The impedance matching measured on the Smith chart for this antenna was 50 Ω, approximately, and the result is presented in Fig. 8. The voltage standing wave ratio (VSWR) curve measurements are shown in the Fig. 9.

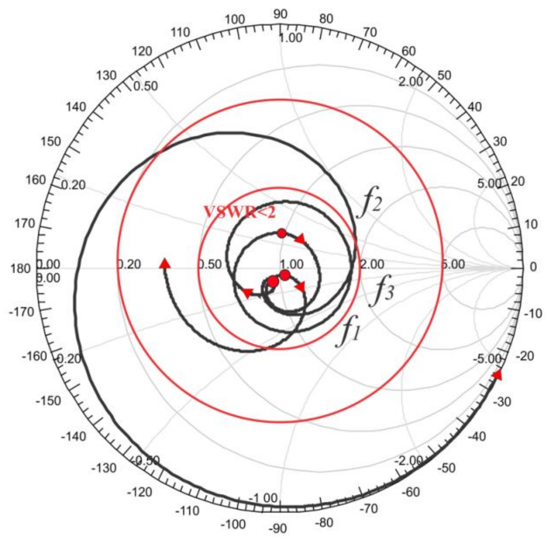

Fig. 8. Input Impedance simulated of the PMA "*Elliptical Camellia*" for W_2.

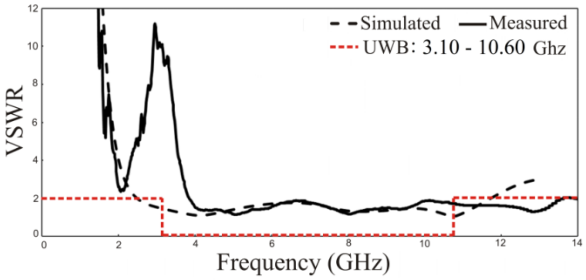

Fig. 9. VSWR curve measurements of PMA "*Elliptical Camellia*" for W_2.

Fig. 10 shows the normalized current density in A/m^2 for the resonance frequencies presented on the Fig. 3 and 4. As expected, it can be noted that the surface current distribution at the edges is higher than in the center of the printed monopole antenna.

The PMA antenna based on the Elliptical Camellia curve shows a current density J in between J_1 = 5.1449 – 0.0018 A/m^2 for f_1 = 4.1392 GHz (Fig. 11.a), J_2 = 1.694 – 0.058 A/m^2 for f_2 = 8.3980 GHz (Fig. 11.b), and J_3 = 19.6 – 0.026 A/m^2 for f_3 = 10.7371 GHz (Fig. 11.b), respectively, with a better distribution for the last one. We note that the PMA W_2 has presented a good current distribution in the patch element, indicating a structure with improved energy utilization.

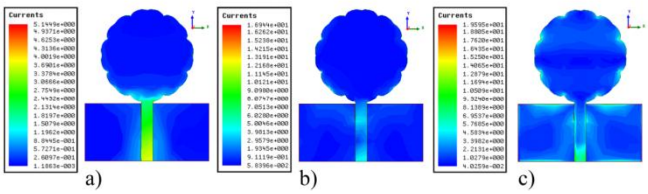

Fig. 10. Current density in A/m^2 for the PMA: a) $\boldsymbol{f_1}$ **=** 4.1392 GHz**.** b) f_2 = 8.3980 GHz. c) f_3 = 10.7371 GHz**.**

IV. CONCLUSIONS

In this work, the design of a printed monopole antenna (PMA) with low losses has been investigated numerically and experimentally where the antenna's characteristics are suitable for UWB applications. The bioinspired PMA was designed for UWB and X-Band ranges, which is based on the geometry of the camellia flower. The antenna demonstrated low return loss, consequently a good impedance matching, and a parametric study of the ground plane width allowed an improvement in the performance of the PMA for the proper UWB operation. Good radiation characteristics with directional radiation pattern were observed and the characteristic current modes on the antenna are identified and provide insights into the antenna properties, which was constructed and analyzed. The next step of this work is the construction of arrays using precision techniques, such as 3D printing, to verify the agreement between measured and simulated data.

ACKNOWLEDGEMENTS

The authors thanks the support of CNPq under covenant 472098/2013-6, State University of Paraíba (UEPB), Federal University of Campina Grande (UFCG) and Federal Institute of Paraíba (IFPB).

REFERENCES

[1] Narayan Prasad Agrawall, Girish Kumar, and K. P. Ray, "Wide-Band Planar Monopole Antennas, IEEE Transactions on Antennas and Propagation", vol. 46, no. 2, February 1998, pp. 294-295.
[2] A. Bekasiewicz, and S. Koziel, "A Concept and Design Optimization of Compact Planar UWB Monopole Antenna", IEEE Int. Sym. Ant. Prop., pp. 1813-1814, 2014.
[3] Bao, X.L.; Ammann, M.J.: "Investigation on UWB printed monopole antenna with rectangular slitted ground plane". Microw. Opt.Technol. Lett. 49(7), 1585–1587 (2007).
[4] Integrated Publishing: http://electriciantraining.tpub.com/14182/
[5] R. Azim, M. T. Islam, N. Misran, "Microstrip Line-fed Printed Planar Monopole Antenna for UWB Applications", Arab. J. Sci. Eng. (2013), 38:2415–2422.
[6] R. Soorya, K. Ramprakash, "UWB microstrip patch antenna with flower shaped patch and cavity structure", IEEE WiSPNET 2016 Conference", DOI: 10.1109/WiSPNET.2016.7566508.
[7] K. Falconer, "Fractal geometry: mathematical foundations and applications", 2nd ed., Wiley, London, 2003.
[8] J. Gielis, "A generic geometric transformation that unifies a wide range of natural and abstract shapes", American Journal of Botany 90(3): 333–338. 2003.
[9] C. A. Balanis, "Antenna theory: analysis and desing". 2 ed Wiley, 1997.
[10] Photosynthetic Antenna Research Center, Theme 1: "Natural Antennas: Structure & Efficiency". https://parc.https://parc.wustl.edu/research/themes/natural (Avaiable).
[11] Goldstein, Hebert; Classical Mechanics - Second Edition; Addison-Wesley Publishing Company; 1922 ; ISBN 0-201-02918-9.
[12] K. G. Thomas and M. Sreenivasan, "A Simple Ultrawideband Planar Rectangular Printed Antenna With Band Dispensation," IEEE Transactions on Antennas and Propagation, Vol. 58, No. 1, 2010, pp. 27-34.
[13] H. J. Lak, C. Ghobadi and J. Nourinia, "A Novel Ultra-Wideband Monopole Antenna with Band-Stop Characteristic," Wirelles Engineering and Technology, 2011, 2, 235-239.
[14] N. C. Azenui and H. Y. D. Yang, "A Printed Crescent Patch Antenna for Ultrawideband Applications," IEEE Antennas and Wireless Propagation Letters, VOL. 6, 2007.